J Fluoresc (2009) 19:151–157
DOI 10.1007/s10895-008-0396-0

ORIGINAL PAPER

Studies on Interaction of CdTe Quantum Dots with Bovine Serum Albumin Using Fluorescence Correlation Spectroscopy

Liwen Shao · Chaoqing Dong · Fuming Sang · Huifeng Qian · Jicun Ren

Received: 30 September 2007 / Accepted: 23 June 2008 / Published online: 8 July 2008

Abstract Luminescent quantum dots (QDs) have widely used in some biological and biomedical fields due to their unique and fascinating optical properties, meanwhile the interaction of QDs with biomolecules recently attract increasing attention. In this paper, we employed fluorescence correlation spectroscopy (FCS) to investigate the nonspecific interaction between CdTe QDs and bovine serum albumin (BSA) as a model, and evaluate their stoichiometric ratio and association constant. Our results documented that BSA was able to bind to CdTe QDs and form the QD–BSA complex by a 1:1 stoichiometric ratio. The association constant evaluated is $1.06\pm0.14\times10^7$ M^{-1} in 0.01 M phosphate buffer (pH=7.4). Furthermore, we found that QD–BSA complex dissociated with increase of ion strength, and we speculated that the interaction of CdTe QDs with BSA was mainly attributed to electrostatic attraction. Our preliminary results demonstrate that fluorescence correlation spectroscopy is an effective tool for investigation of the interaction between quantum dots (or nanoparticles) and biomolecules.

Keywords CdTe · BSA · Interaction · Fluorescence correlation spectroscopy

Introduction

Recently luminescent quantum dots (QDs) are gaining tremendous interest in biological and biomedical fields because of their unique and fascinating properties, such as tunable emission wavelength, broad absorption and sharp emission spectra, high quantum yield (QY), resistance to the chemical degradation and photobleaching, and versatility in surface modification [1–3]. Some water-soluble QDs conjugated with biomolecules were successfully used in fluorescent resonance energy transfer (FRET), in vivo and vitro imaging, immunoassay, DNA hybridization, and potential photodynamic therapy [4–10]. However, the interaction of QDs with biomolecules is very little known, which is very important to know the bioeffects of QDs. So far, some analytical techniques, such as atomic force microscopy (AFM), gel electrophoresis, dynamic light scattering (DLS), size-exclusion high-performance liquid chromatography (SE-HPLC), and circular dichroism spectroscopy (CD), have been tried to study the interaction of QDs with biomolecules [4, 11–17]. But these current techniques are still difficult to obtain some important information on the interaction of QDs with biomolecules such as binding constant. Particularly, the experimental evaluations of some parameters like stoichiometry and association constant, which are the fundamental prerequisite for QD bio-applications, are rarely reported. In general, the stoichiometry of QD bioconjugation was calculated theoretically according to the structures of QDs and ligands, but the effects of their steric hindrance was not considered in this approach [18]. Recent notable works were carried out for characterization of the stoichiometry of QD conjugates using the techniques mentioned above [12–14]. Especially, Lindman and Cedervall reported a noteworthy study on the hydrophobic interaction between large size nanoparticles and biomolecules [19, 20]. They obtained the stoichiometry and thermodynamic parameters for adsorption of human serum albumin to copolymer nanoparticles using isothermal titration calorimetry.

L. Shao · C. Dong · F. Sang · H. Qian · J. Ren (✉)
College of Chemistry and Chemical Engineering,
Shanghai Jiaotong University,
800 Dongchuan Road,
Shanghai 200240, People's Republic of China
e-mail: jicunren@sjtu.edu.cn

Fluorescence correlation spectroscopy (FCS) is an ultrasensitive and noninvasive single molecule detection technique that uses statistical analysis of the fluctuations of fluorescence emitted from a small, optically well-defined open volume element [21, 22]. Some important information, such as the average number of luminescent particles in the volume and the coefficient of diffusion, can be obtained by the autocorrelation function (ACF), and the changes of ensemble luminescence intensity and the brightness per particle (BPP) can be measured based on count rate and the number of bright particles [23]. So far, this method has been successfully used in some fields such as DNA hybridization, immunoassay and single cell analysis, and has become a useful analytical technique to evaluate the kinetics and thermodynamics parameters of biomolecule interaction [24–27]. Recently, FCS was also used to characterize some important parameters of QDs, including their concentration, brightness, hydrodynamic radius, and monodispersity [28–32]. In this work, we want to explore the possibility of investigation on interaction of QDs and proteins by FCS. In this study, CdTe QDs and bovine serum albumin (BSA) were used as model samples. We observed that BSA easily adsorbed to the surface of CdTe QDs in phosphate buffer. Importantly, no significant change of the absorption and emission spectra of BSA and CdTe QDs mixtures occurred compared to free CdTe QDs. The interaction of BSA with CdTe QD was able to be characterized by FCS, and the stoichiometric ratio and association constant of CdTe QD–BSA complex were obtained by the one-component and two-component fit of ACF.

Experimental section

Materials and reagents Rhodamine 6G and Alexa Fluor succinimidyl esters (Alexa647) were purchased from Molecular Probes (Eugene, OR). Bovine serum albumin (BSA), Rhodamine B isothiocyanate (RBITC) and mercaptopropionic acid (MPA) were obtained from Aldrich-Chemie (Steinheim, Germany). All other chemicals used in this study were of the highest purity available and purchased from regular sources. All solutions were prepared with ultrapure water purified on Millipore Simplicity (Millipore, USA), and filtered through 0.22 μm membrane filters (Shanghai Bandao Co., China) prior to use.

Preparation and characterization of CdTe QDs Water-soluble CdTe quantum dots was synthesized according to the procedure reported elsewhere [33]. The as-prepared products were precipitated with 2-propanol to remove free Cd^{2+} and MPA, and the approach was described in the reference [34]. Emission spectra were recorded using a Varian Cary spectrometer, and absorption spectra were obtained by a Lambda 20 UV-visible spectrophotometer (Perkin-Elmer). The QY of CdTe QDs was measured according to the method described in the references [34]. The absorption peak position and the emission peak position of CdTe QDs used here were at 576 nm and 608 nm respectively, and the QY of CdTe QDs was about 50%.

Conjugation and purification approaches BSA was conjugated to CdTe QDs by nonspecific attraction. Typically, certain concentration QDs solutions were titrated with the different volume of BSA solution in 0.01 M phosphate buffer (pH=7.4). The reactions were carried out at room temperature for 3~4 h. The mixtures were diluted to the concentration of 0.25 μM in CE procedure and 50 nM in FCS measurement. Certain labeling mixtures were purified with the YM-100 ultra-filtration membrane (NMWL 100 000, Millipore, USA) according to the procedure in the reference in order to obtain the pure QD–BSA complex. Meanwhile, RBITC was used to label BSA in order to determine size of BSA. The ratio of RBITC to BSA was 1:10 approximately, and the YM-10 ultra-filtration membrane (NMWL 10 000) was used to remove the free RBITC. Besides, in order to prepare amount of Alexa647-labeled BSA, BSA was reacted with Alexa647 with the 1:10 ratio of BSA to Alexa647 to ensure that every BSA molecule was labeled with Alexa647. The free Alexa647 was removed by the YM-30 ultra-filtration membrane (NMWL 30 000).

Capillary electrophoresis procedure A P/ACE MDQ capillary electrophoresis system (Beckman Counter, Fullerton, CA, USA) with LIF detector was employed, and Ar ion laser (488 nm) was used as the exciting light source. Fused-silica capillaries were purchased from Yongnian Optical Fiber Co. (Hebei, China). In this study, CE was used to characterize the QD and QD–BSA complex.

The CE was performed under a normal polarity separation mode. A 40 cm capillary with 30 cm effective length and inner diameter (I.D.) of 75 μm was used for the characterization of the QD and QD–BSA complex. The new capillary was rinsed successively with 0.1 M NaOH for 10 min, water for 3 min, 0.1 M HCl for 10 min, then with water for 3 min and finally with running buffer (6.25 mM borate buffer, pH=10) for 5 min. The samples were introduced into the capillary by pressure (0.5 psi) for 4 s. The applied voltage was 12 kV, and the temperature of the separation capillary column was thermostated at 25°C. Between each measurements, the capillary was rinsed with 0.1 M NaOH for 5 min, and then with the electrophoresis buffer for 3 min.

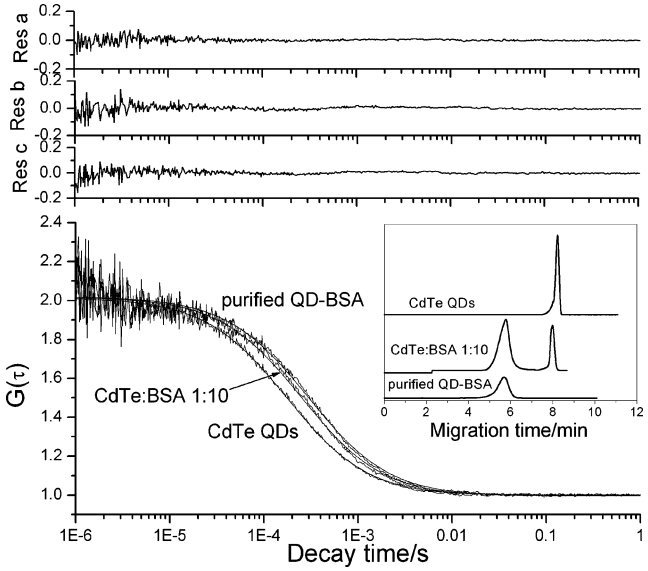

Fig. 1 Normalized autocorrelation functions and their fitting curves of CdTe QDs, a mixture by a 1:10 molar ratio (QD:BSA), and purified QD–BSA complex *from left to right* respectively. The *inset* depicts the corresponding electrophoregrams of CdTe QDs, a mixture by a 1:10 molar ratio (QD:BSA), and purified QD–BSA complex. The residuals of three fitted correlation curves are shown as "*Res a*", "*Res b*" and "*Res c*" standing for fit residuals of CdTe QDs, a mixture by a 1:10 molar ratio (QD:BSA), and purified QD–BSA complex, respectively

Fluorescence correlation spectroscopy measurement Fluorescence Correlation Spectroscopy (FCS) measurements were performed with a home-built FCS system [35]. In brief, for QD and its protein hybrid, the 543 nm laser line from a He–Ne ion laser (Coherent, USA.) was attenuated to about 40 μW by a circular neutral density filter, and then expanded to underfill the back aperture of the objective lens. The expanded laser beam was focused with a water immersion objective (UplanApo, 60×NA1.2, Olympus, Japan) to a small volume within the diluted sample. The resulting excitation volume is on the order of 1 fL. The excited fluorescence signal collected by the objective passed through the dichroic mirror (570DRLP, Omega Optical, USA) and then was filtered by a band-pass filter (605DF50, Omega Optical, USA) to block scattering laser light. Finally, the fluorescence was coupled into a 35-μm pinhole at the image plane in front of the single-photon counting module (SPCM-AQR16, Perkin-Elmer EG and G, Canada). The fluorescence fluctuations were correlated with a digital correlator (Flex02-12D/C, Correlator.com, USA).

For the measurements of Alexa647 labeled samples, the 632.8 nm He–Ne laser (Hongyang, China), 660DF50 band-pass filter (Omega Optical, USA), 650DRLP dichroic mirror (Omega Optical, USA) were employed.

All raw FCS data were analyzed with the standard equation for multi-component model (Eq. 1) and non-linearly fitted with the Microcal Origin 6.0 software package based on the Levenberg−Marquardt algorithm:

$$G(\tau) = \frac{1}{N}\left(1 + \frac{T}{1-T}e^{-\tau/\tau_{tr}}\right) \sum_{i=1}^{K} \frac{y_i}{1+\frac{\tau}{\tau_i}} \frac{1}{\left(1+\left(\frac{\omega_0}{z_0}\right)^2 \frac{\tau}{\tau_i}\right)^{\frac{1}{2}}} + 1 \quad (1)$$

where N is the average number of fluorescent particles diffusing in the focused volume. T is the fraction of the fluorescent particles in triplet state (for QDs T=0) whose lifetime is τ_{tr}. y_i is the fraction of the ith fluorescent component. ω_0 and z_0 are the transverse and axial radii of the focus volume respectively. τ_i is the characteristic diffusion time of the ith component. The Eq. 1 is valid when the quantum yield of free and labeling fluorescent particles are the same. The characteristic diffusion time of the ith component is defined as

$$\tau_i = \frac{\omega_0^2}{4D_i} \quad (2)$$

Where D_i is the diffusion constant, and can be obtained by calibrating with the standard substance (Eq. 3). In our experiments, R6G and Alexa647 are used as the standard substances. The diffusion coefficient of R6G and Alexa647 are both 2.8×10^{-6} cm^2/s [35, 36].

$$D_i = \frac{\tau_{R6G}}{\tau_i} D_{R6G} \quad (3)$$

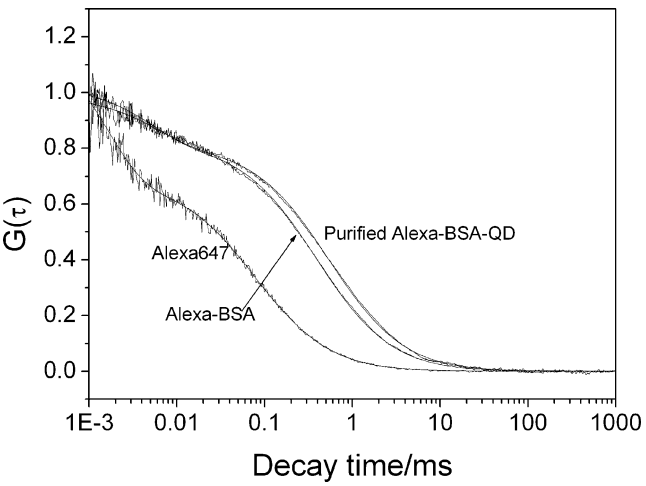

Fig. 2 One-component fits to the experimental ACFs for Alexa647, Alexa-BSA and Alexa-BSA-QD. All functions are normalized for clarity. Their corresponding BPPs are 16.3 kHz (*Alexa647*), 43.6 kHz (*Alexa-BSA*), and 46.9 kHz (*Alexa-BSA-QD*), respectively

For spherical particle D is inversely proportional to its hydrodynamic radius according to the Stokes–Einstein equation

$$D = \frac{kT}{6\pi\eta r} \tag{4}$$

where kT is the thermal energy and η is the viscosity. The hydrodynamic radius (r) of the fluorescent particle can be obtained by the diffusion constant consequently.

Results and discussion

Determination of stoichiometric ratio

In this study, water-soluble CdTe quantum dots were synthesized using cadmium salts and NaHTe as precursors in the presence of MPA as stabilizer. Prior to study on interaction of QDs and protein, CdTe QDs were precipitated with 2-propanol to remove free Cd^{2+}, which was known to easily react with disulfide bridges in BSA and denature the protein. Figure 1 shows the nice normalized ACFs of free CdTe QD, a mixture and QD–BSA complex, respectively. The results demonstrated that free CdTe QD and QD–BSA complex had significantly different diffusion time, which demonstrated that BSA was able to adsorb to BSA. In experiments, the QD–BSA complex was purified from QDs and BSA reaction mixture with the YM-100 ultra-filtration membrane. The CE (as shown in Fig. 1) further proved that there were no free QDs in the purified QD–BSA complex. The measured characteristic diffusion time of CdTe QD was 171±2 μs (n=10) with the brightness per particle (BPP) of 11.5 kHz, whose corresponding hydrodynamic diameter was 4.4±0.1 nm. This result was basically in agreement with the size measured by the transmission electron spectroscopy (TEM). The ACF fitting results indicated that the characteristic diffusion time of QD–BSA complex was 296±4 μs with BPP of 9.9 kHz, whose corresponding hydrodynamic diameter was 7.6± 0.2 nm. Meanwhile, the hydrodynamic diameter of BSA labeled with RBITC was evaluated to 5.6±0.1 nm by FCS. By comparing the hydrodynamic diameters of QD–BSA complex with CdTe QDs and BSA, we preliminarily deduced that one BSA molecule was attached with a single CdTe QD. Nevertheless, the hydrodynamic diameter of QD–BSA complex was not completely in agreement with the theoretically summed value of the diameters. This phenomenon is probably due to non-spherical shapes of BSA and QD–BSA complex. In the evaluation of hydrodynamic diameter according to Einstein formula, normally the BSA and QD–BSA complex were regarded as a spherical shape.

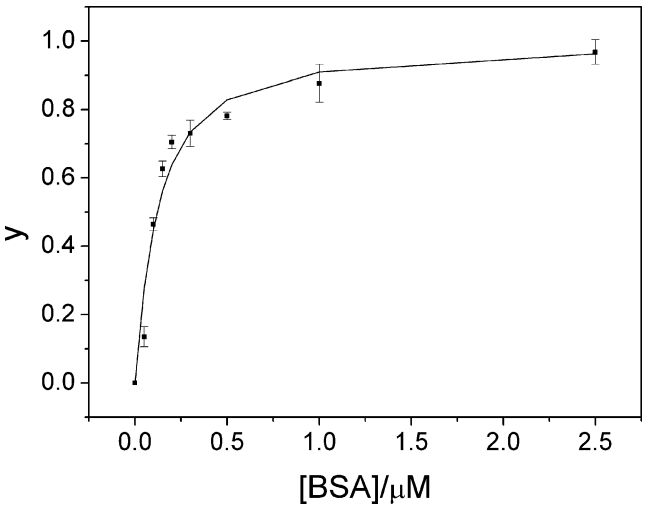

Fig. 3 The titration curve of FCS measurement depending on the concentration of BSA derived from the fits of ACF at a QD concentration of 50 nM

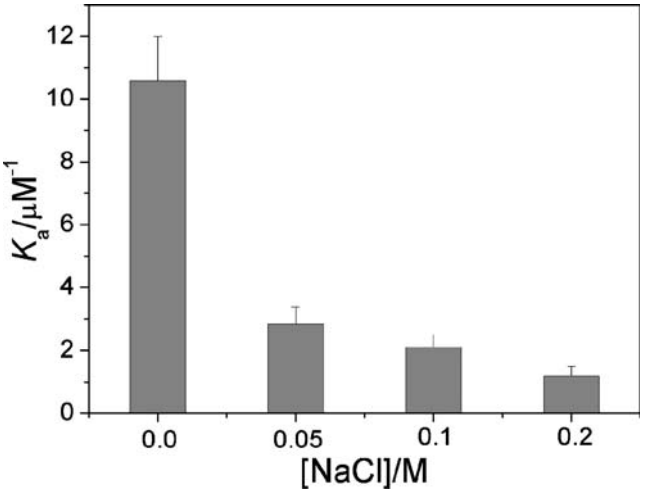

Fig. 4 Effects of NaCl concentrations on the association constant. *Error bars* are standard deviations

In order to further confirm the stoichiometry determination based on the hydrodynamic radius, the reverse titration was conducted. Here, the Alexa-BSA hybrid as probe was applied to titrate CdTe QD. The experiments were carried out with 632.8 nm He–Ne laser. The ACFs of Alexa647, Alexa-BSA and the complex of CdTe QD and labeled BSA are depicted in Fig. 2. It is noteworthy that about 2~3 Alexa647 molecules were conjugated to one BSA molecule from BPP comparison, and Alexa647-BSA and Alexa647-BSA-CdTe have comparable BPP (43.6 kHz for Alexa647-BSA and 46.9 kHz for Alexa647-BSA-CdTe). The result firmly supported the 1:1 conjugation of CdTe QD with BSA.

Evaluation of association constant

As shown in the above section, the conjugation of QDs and BSA can be described by a 1:1 stoichiometric ratio.

$$QD + BSA \rightleftharpoons QD - BSA \tag{5}$$

The percentage of the QD–BSA complex (y) can be acquired with FCS, which is defined as:

$$y = \frac{[\mathrm{QD} - \mathrm{BSA}]}{[\mathrm{QD}] + [\mathrm{QD} - \mathrm{BSA}]} \tag{6}$$

The dissociation constant (K_d) can be defined as:

$$K_d = \frac{[\mathrm{QD}][\mathrm{BSA}]}{[\mathrm{QD} - \mathrm{BSA}]} \tag{7}$$

where [QD] and [BSA] are the concentrations of free QDs and BSA respectively, and [QD–BSA] is the concentration of QD–BSA complex. From the Eqs. 6 and 7, y can be express as:

$$y = \frac{\left(K_d + c_{\mathrm{QDs}} + c_{\mathrm{BSA}}\right)}{2c_{\mathrm{QDs}}} - \left(\left(\frac{K_d + c_{\mathrm{QDs}} + c_{\mathrm{BSA}}}{2c_{\mathrm{QDs}}}\right)^2 - \frac{c_{\mathrm{BSA}}}{c_{\mathrm{QDs}}}\right)^{\frac{1}{2}} \tag{8}$$

where c_{QDs} and c_{BSA} stand for the initial concentration of QDs and BSA, and y is determined from each titration point in FCS measurement. For all evaluations of K_d, this titration curve was fitted by Levenberg–Marquardt algorithm of the Microcal Origin 6.0 software package with the fixed QD concentration. The association constant (K_a) is the reciprocal of the K_d.

Herein, FCS was employed to evaluate the association constant of interaction of QDs with BSA. The equilibrium of association reaction reached in 2 h (determined by FCS, and the characteristic diffusion time of the mixture became constant in 2 h). The characteristic diffusion time of CdTe QD and QD–BSA complex determined in the above FCS measurements, were different by more than a factor of 1.6 (τ_{CdTe}=171±2 μs and τ_{complex}=296±4 μs). Meanwhile, we observed that luminescence intensity per QD–BSA complex was comparable to those of per QD (11.4 kHz for BPP of CdTe QD and 9.9 kHz for BPP of QD–BSA complex). These data suggest us that two-component fitting procedure can be used to distinguish the two different components of QDs and QD–BSA complex [37]. In two-component fitting, the characteristic diffusion times of CdTe QD and QD–BSA complex were fixed. The titration curve of percentage of the QD–BSA complex (y) vs. the concentration of BSA is depicted in Fig. 3 based on the results by fitting two-component fit procedure. In the fit procedure, the characteristic diffusion time increased with BSA concentration, indicating the formation of QD–BSA complex. A fit with Eq. 8 gave a value of $9.44\pm1.25\times10^{-8}$ M for the dissociation constant at room temperature (about 20°C). The corresponding association constant was $1.06\pm0.14\times10^{7}$ M^{-1}.

Influences of ion strength

Nonspecific interaction usually includes electrostatic attraction and hydrophobic force. Goldman et al. investigated the interaction of QDs with avidin, NeutrAvidin and Strepavidin, and they believed that the conjugation of QDs with avidin was attributed to charge–charge interaction [38]. Ha et al. immobilized esterase onto 16-mercapto- hexadecanoic acid (MHA) protected gold nanoparticles and observed the existence of both electrostatic attraction and hydrophobic force [39]. In this study, to elucidate the nonspecific interaction of BSA with CdTe QDs, sodium chloride solutions at different concentration (0~0.2 M) were used to investigate the effects of ion strength on the nonspecific interaction with FCS. Here, the influences of sodium chloride (0~0.2 M) on the brightness of QDs and QD–BSA complex were basically neglectable. Fig. 4A depicts the dependence of association constant (K_a) of QD–BSA complex on salt concentration in solution. The value of K_a decreased with the increase of sodium chloride concentration. This preliminary result suggested us that the interaction between QDs and BSA was mainly attributed to their electrostatic attraction.

Conclusion

In this work we studied nonspecific interaction of CdTe QDs and BSA using FCS, and evaluated the stoichiometry and association constant of the CdTe QD–BSA complex. The stoichiometry of QD–BSA conjugation was 1:1 based on the sizes and BPP of the free particles and their complex, and the association constant between CdTe QD and BSA was $1.06\pm0.14\times10^{7}$ M^{-1}. Furthermore, we investigated the effects of the ion strength on the CdTe QD–BSA complex, and found that the complex was dissociated considerately with the increase in the ion strength. We speculated that the nonspecific conjugation of QD with BSA was mainly attributed to the electrostatic attraction. Our preliminary results demonstrate that FCS is a very useful analytical technique for the investigations of the interactions of QDs (or nanoparticles) with biomolecules.

Acknowledgements This work was financially supported by the National Natural Science Foundation of China (No. 20675052, 20727005) and National High-Tech R and D Program (2006AA03Z324)

References

1. Alivisatos AP, Gu WW, Larabell C (2005) Quantum dots as cellular probes. Annu Rev Biomed Eng **7**:55–76, doi:10.1146/annurev.bioeng.7.060804.100432
2. Michalet X, Pinaud FF, Bentolila LA, Tsay JM, Doose S, Li JJ et al (2005) Quantum dots for live cells, in vivo imaging, and diagnostics. Science 307:538–544, doi:10.1126/science.1104274
3. Medintz IL, Uyeda HT, Goldman ER, Mattoussi H (2005) Quantum dot bioconjugates for imaging, labelling and sensing. Nat Mater 4(6):435–446, doi:10.1038/nmat1390
4. Wang Y, Tang Z, Kotov NA (2005) Bioapplication of nano-semiconductors. Mater Today 8(5):20–31, doi:10.1016/S1369-7021(05)00892-8
5. Clapp AR, Medintz IL, Mattoussi H (2006) Forster resonance energy transfer investigations using quantum-dot fluorophores. Chem Phys Chem **7**(1):47–57, doi:10.1002/cphc.200500217
6. Ballou B, Lagerholm BC, Ernst LA, Bruchez MP, Waggoner AS (2004) Noninvasive imaging of quantum dots in mice. Bioconjug Chem 15(1):79–86, doi:10.1021/bc034153y
7. Sun B, Xie W, Yi G, Chen D, Zhou Y, Cheng J (2001) Microminiaturized immunoassays using quantum dots as fluorescent label by laser confocal scanning fluorescence detection. J Immunol Methods 249(1):85–89, doi:10.1016/S0022-1759(00)00331-8
8. Samia ACS, Chen X, Burda C (2003) Semiconductor quantum dots for photodynamic therapy. J Am Chem Soc 125(51):15736–15737, doi:10.1021/ja0386905
9. Pathak S, Choi SK, Arnheim N, Thompson ME (2001) Hydroxylated quantum dots as luminescent probes for in situ hybridization. J Am Chem Soc 123(17):4103–4104, doi:10.1021/ja0058334
10. Wu X, Liu H, Liu J, Haley KN, Treadway JA, Larson JP et al (2003) Immunofluorescent labeling of cancer marker Her2 and other cellular targets with semiconductor quantum dots. Nat Biotechnol 21(1):41–46, doi:10.1038/nbt764
11. Parak WJ, Gerion D, Zanchet D, Woerz AS, Pellegrino T, Micheel C, Seitz SC, Williams M, Bruehl RE, Bryant Z, Bustamante C, Bertozzi CR, Alivisatos AP (2002) Conjugation of DNA to silanized colloidal semiconductor nanocrystalline quantum dots. Chem Mater 14(5):2113–2119, doi:10.1021/cm0107878
12. Nehilla BJ, Vu TQ, Desai TA (2005) Stoichiometry-dependent formation of quantum dot-antibody bioconjugates: a complementary atomic force microscopy and agarose gel electrophoresis study. J Phys Chem B 109(44):20724–20730, doi:10.1021/jp052613+
13. Ipe BI, Shukla A, Lu H, Zou B, Rehage H, Niemeyer CM (2006) Dynamic light-scattering analysis of the electrostatic interaction of hexahistidine-tagged cytochrome P450 enzyme with semiconductor quantum dots. Chem Phys Chem **7**(1):1–8, doi:10.1002/cphc.200690000
14. Pons T, Uyeda HT, Medintz IL, Mattoussi H (2006) Hydrodynamic dimensions, electrophoretic mobility, and stability of hydrophilic quantum dots. J Phys Chem B 110(41):20308–20316, doi:10.1021/jp065041h
15. Mamedova NN, Kotov NA, Rogach AL, Studer J (2001) Albumin-CdTe nanoparticle bioconjugates: preparation, structure, and interunit energy transfer with antenna effect. Nano Lett 1(6):281–286, doi:10.1021/nl015519n
16. Pinaud F, King D, Moore H-P, Weiss S (2004) Bioactivation and cell targeting of semiconductor CdSe/ZnS nanocrystals with phytochelatin-related peptides. J Am Chem Soc 126(19):6115–6123 doi:10.1021/ja031691c
17. Ding S-Y, Jones M, Tucker MP, Nedeljkovic JM, Wall J, Simon MN et al (2003) Quantum dot molecules assembled with genetically engineered proteins. Nano Lett 3(11):1581–1585, doi:10.1021/nl034578t
18. Mattoussi H, Mauro JM, Goldman ER, Anderson GP, Sunder VC, Mikulee FV et al (2000) Self-assembly of CdSe-ZnS quantum dot bioconjugates using an engineered recombinant protein. J Am Chem Soc 122(49):12142–12150, doi:10.1021/ja002535y
19. Lindman S, Lynch I, Thulin E, Nilsson H, Dawson KA, Linse S (2007) Systematic investigation of the thermodynamics of HSA adsorption to N-iso-propylacrylamide/*N*-tert-butylacrylamide copolymer nanoparticles. effects of particle size and hydrophobicity. Nano Lett **7**(4):914–920, doi:10.1021/nl062743+
20. Cedervall T, Lynch I, Linderman S, Berggard T, Thulin E, Nilsson H et al (2007) Understanding the nanoparticle-protein corona using methods to quantify exchange rates and affinities of proteins for nanoparticles. Proc Natl Acad Sci U S A 104(7):2050–2055, doi:10.1073/pnas.0608582104
21. Hess ST, Huang SH, Heikal AA, Webb WW (2002) Biological and chemical applications of fluorescence correlation spectroscopy: a review. Biochemistry 41(3):697–705, doi:10.1021/bi0118512
22. Haustein E, Schwille P (2003) Ultrasensitive investigations of biological systems by fluorescence correlation spectroscopy. Methods 29(2):153–166, doi:10.1016/S1046-2023(02)00306-7
23. Dong CQ, Qian HF, Fang NH, Ren JC (2006) Study of fluorescence quenching and dialysis process of CdTe quantum dots, using ensemble techniques and fluorescence correlation spectroscopy. J Phys Chem B 110(23):11069–11075, doi:10.1021/jp060279r
24. Wohland T, Friedrich K, Hovius R, Vogel H (1999) Study of ligand–receptor interactions by fluorescence correlation spectroscopy with different fluorophores: evidence that the homopentameric 5-hydroxytryptamine type 3as receptor binds only one ligand. Biochemistry 38(27):8671–8681, doi:10.1021/bi990366s
25. Schubert F, Zettl H, Hafner W, Krauss G, Krausch G (2003) Comparative thermodynamic analysis of DNA–protein interactions using surface Plasmon resonance and fluorescence correlation spectroscopy. Biochemistry 42(34):10288–10294, doi:10.1021/bi034033d
26. Ling CH, Gosch M, Lasser T, Wohland T (2006) Simultaneous multicolor fluorescence cross-correlation spectroscopy to detect higher order molecular interactions using single wavelength laser excitation. Biophys J 91(2):715–727, doi:10.1529/biophysj.105.074120
27. Pack C-G, Aoki K, Taguchi H, Yoshida M, Kinjo M, Tamura M (2000) Effect of electrostatic interactions on the binding of charged substrate to GroEL studied by highly sensitive fluorescence correlation spectroscopy. Biochem Biophys Res Commun 267(1):300–304, doi:10.1006/bbrc.1999.1864
28. Larson DR, Zipfel WR, Williams RM, Clark SW, Bruchez MP, Wise FW et al (2003) Water-soluble quantum dots for multiphoton fluorescence imaging in vivo. Science 300:1434–1436, doi:10.1126/science.1083780
29. Doose S, Tsay J, Pinaud F, Weiss S (2005) Comparison of photophysical and colloidal properties of biocompatible semiconductor nanocrystals using fluorescence correlation spectroscopy. Anal Chem 77(7):2235–2242, doi:10.1021/ac050035n
30. Yao J, Larson DR, Vishwasrao HD, Zipfel WR, Webb WW (2005) Blinking and nonradiant dark fraction of water-soluble quantum dots in aqueous solution. Proc Natl Acad Sci USA 102(40):14284–14298, doi:10.1073/pnas.0506523102
31. Tsay JM, Doose S, Pinaud F, Weiss S (2005) Enhancing the photoluminescence of peptide-coated nanocrystals with shell composition and UV irradiation. J Phys Chem B 109(5):1669–1674, doi:10.1021/jp046828f
32. Pellegrino T, Manna L, Kudera S, Liedl T, Koktysh D, Rogach AL, Keller S, Raedler J, Natile G, Parak WJ (2004) Hydrophobic nanocrystals coated with an amphiphilic polymer shell: a general route to water soluble nanocrystals. Nano Lett 4(4):703–707, doi:10.1021/nl035172j

33. Li L, Qian HF, Ren JC (2005) Rapid synthesis of highly luminescent CdTe nanocrystals in the aqueous phase by microwave irradiation with controllable temperature. Chem Commun (Camb) 528–530, doi:10.1039/b412686f
34. Li L, Qian HF, Fang NH, Ren JC (2006) Significant enhancement of the quantum yield of CdTe nanocrystals synthesized in aqueous phase by controlling the pH and concentrations of precursor solutions. J Lumin 116(1):59–66, doi:10.1016/j.jlumin.2005.03.001
35. Zhang PD, Li L, Dong CQ, Qian HF, Ren JC (2005) Sizes of water-soluble luminescent quantum dots measured by fluorescence correlation spectroscopy. Anal Chim Acta 546(1):46–51, doi:10.1016/j.aca.2005.05.034
36. Wang KL, Qiu X, Dong CQ, Ren JC (2007) Single-molecule technology for rapid detection of dna hybridization based on resonance light scattering of gold nanoparticles. Chem Bio Chem 8(10):1126–1129, doi:10.1002/cbic.200700174
37. Meseth U, Wohland T, Rigler R, Vogel H (1999) Resolution of fluorescence correlation measurements. Biophys J 76(3):1619–1631
38. Goldman ER, Balighian ED, Mattoussi H, Kuno MK, Mauro JM, Tran PT et al (2002) Avidin: a natural bridge for quantum dot-antibody conjugates. J Am Chem Soc 124(22):6378–6382, doi:10.1021/ja0125570
39. Ha TH, Jeong JY, Chung BH (2005) Immobilization of hexa-arginine tagged esterase onto carboxylated gold nanoparticles. Chem Commun (Camb) 3959–3961, doi:10.1039/b504184h